and comparable, albeit slightly smaller, to those of **1** ($|D|$ = 144 and $|E|$ = 5.0 G). Furthermore, the spectrum measured at 100 K shows the fine structure also in the central signal. The $|D|$ value is ca. 5 G.[29] The intensity of the triplet signals gradually decreases if the temperature is lowered from 293 to 50 K, obviously implying that the triplet state is thermally accessible. The temperature dependence of the signal intensity obeys an equation of $I = N_b\mu_B^2g^2[1(1+1)][3kT\{1+{}^1/_3\exp(\Delta E/kT)\}]$, where I is the triplet signal intensity, N_b the amount of biradical, μ_B the Bohr magneton, k the Boltzmann constant, and ΔE the energy gap between the singlet and the higher triplet. ΔE was estimated to be ca. 1.3 kcal/mol. On the other hand, the intensity of the central signal increased with lowering the temperature from 293 to 130 K and then reversely decreased in the temperature range lower than 130 K. According to an equation relating the signal intensity with temperature for a thermally-accessible triplet contaminated with an impurity monoradical, $I = N_m\mu_B^2g^2[{}^1/_2(1+{}^1/_2)/3kT] + N_b\mu_B^2g^2[1(1+1)]/[3kT\{1+{}^1/_3\exp(\Delta E/kT)\}]$ (N_m, monoradical amount), and by counting the exact spin amount of the signal with a reference TANOL, both N_b and ΔE were determined to be 3.9 $\times 10^{20}$ molecules/mol and ca. 0.5 kcal/mol, respectively. This thermally-accessible triplet has a smaller ΔE value compared with that of the triplet first described, suggesting a weaker spin–spin interaction. The observed N_b value indicates an unusually large biradical contribution of 0.07% to the ground state of **2**.[30] This molecule is unique as a closed-shell system. Indeed, two different spin–spin interactions occur in the single microcrystallines of **2**: one is the strong interaction with ΔE = ca. 1.3 kcal/mol, $|D|$ = 93, and $|E|$ = 7.4 G, and the other one is comparatively weaker (ΔE = ca. 0.5 kcal/mol and $|D|$ = ca. 5 G). It is concluded that the interactions are inter- and intramolecular, respectively, in view of the observation of only the $|D|$ = ca. 5 G triplet resonance signals in a polycrystalline sample of **2**, which is obtained by recrystallization from $CHCl_3$/*n*-hexane. In order to support this conclusion, the distance (R) between the two spins in interaction was roughly calculated from the observed $|D|$ value by using a point-dipole approximation, $R = \{{}^3/_2(g\mu_B/|D|)\}^{1/3}$ and comparing with that obtained by the X-ray structure analysis. The R values corresponding to $|D|$ = 93 and ca. 5 G, are 6.7 and ca. 17.7 Å, respectively. The calculated values are consistent with the adjacent O–O distance (7.29 Å) between the two neighboring molecules and with the long-axis distance (15.54 Å) in the molecule, respectively.

The experimental evidence presented here is apropos to the interpretation of the ESR results of **1**. Since **1** has almost the same long-axis distance as **2**, the fine structure due to the interaction between the two spins residing in the molecule should be hidden under the strong monoradical signal of the impurity. Consequently, the triplet resonance signals with a splitting of 288 G can be considered to be caused by the spin–spin interaction between the two neighboring molecules of **1**. The fact that the signals appeared in the polycrystalline sample, but not in single crystals (contrary to **2**), reflects the necessity of molecular stacking to make significant intermolecular spin–spin interactions.

Acknowledgment. This work was supported by the Grant-in-Aid for Scientific Research on Priority Area of Organic Unusual Valency No. 03233101 from the Ministry of Education, Science and Culture, Japan. We are grateful to Prof. K. Takahashi (Tohoku University) for a supply of a compound analogous to **2** prepared by her group.

Registry No. 1, 3624-94-0; **2**, 117474-91-6.

Supplementary Material Available: ORTEP drawing and full tables of fractional atomic coordinates and interatomic bond distances in **2** (4 pages). Ordering information is given on any current masthead page.

(29) The $|E|$ value could not be determined because of overlap between the triplet resonance signals and the impurity monoradical signal.

(30) The degree of biradical contribution to the ground state is unusually large, considering that the biradical is in an electronically-excited singlet state and its thermally-accessible triplet state lies ca. 0.5 kcal/mol above.

Peptide Nucleic Acids (PNA). Oligonucleotide Analogues with an Achiral Peptide Backbone[1]

Michael Egholm,*[†] Ole Buchardt,*[†] Peter E. Nielsen,[‡] and Rolf H. Berg[§]

Research Center for Medical Biotechnology
Chemical Laboratory II, The H. C. Ørsted Institute
University of Copenhagen, Universitetsparken 5
DK-2100 Copenhagen Ø, Denmark
Department of Biochemistry B
The Panum Institute, Blegdamsvej 3
DK-2200 Copenhagen N, Denmark
Polymer Group, Materials Department
Risø National Laboratory
DK-4000 Roskilde, Denmark

Received September 27, 1991

Oligonucleotides that specifically recognize messenger RNA[2-6] or double-stranded DNA present unique opportunities for inhibiting protein synthesis (the antisense approach) or for modulating gene expression, e.g., via triple helix formation.[7,8]

The deoxyribose phosphate backbone of DNA has been modified in a number of ways to increase nuclease stability and cell membrane permeability, assuming that major changes would be deleterious to the "DNA hybridization properties". Consequently, derivatives such as mono-[9,10] or dithiophosphates,[11] methyl phosphonates,[12] borano phosphates,[13] etc.,[4] as well as formacetal,[14] carbamate,[15,16] and siloxane,[17] or dimethylenethio-, -sulfoxido-, and -sulfono-linked[18,19] species were prepared.

The synthesis of peptides is more versatile than oligonucleotide synthesis, allowing the facile design of an achiral backbone and relatively large-scale production. We therefore designed peptide nucleic acids (PNA), i.e., molecules where the individual nucleobases were linked to an achiral peptide backbone.

A suitable distance between nucleobases was estimated by detaching the backbone of one strand in a B-DNA duplex in a computer model and replacing it with amino acid units. The optimal number of bonds between the nucleobases was found to be six, which corresponds to that found in DNA (**1**, Scheme I), and the optimal number of bonds between the backbone and nucleobase to be two to three. This indicated that a backbone

[†] The H. C. Ørsted Institute.
[‡] The Panum Institute.
[§] Risø National Laboratory.

(1) Abbreviations and symbols used (standard oligopeptide nomenclature is used): H-, deprotected terminal amino group; -NH_2, C-terminal amido group; aeg, (2-aminoethyl)glycine; DMF, *N,N*-dimethylformamide; Boc, *tert*-butoxycarbonyl; Pfp, pentafluorophenyl.

(2) Zamecnik, P. C.; Stephenson, M. L. *Proc. Natl. Acad. Sci. U.S.A.* **1978**, *75*, 280–284.
(3) Stephenson, M. L.; Zamecnik, P. C. *Proc. Natl. Acad. Sci. U.S.A.* **1978**, *75*, 285–288.
(4) Uhlmann, E.; Peyman, A. *Chem. Rev.* **1990**, *90*, 544–584.
(5) Hélène, C.; Toulmé, J. *Biochim. Biophys. Acta* **1990**, *1049*, 99–125.
(6) Goodchild, J. *Bioconjugate Chem.* **1990**, *1*, 165–187.
(7) Moser, H. E.; Dervan, P. B. *Science* **1987**, *238*, 645–650.
(8) Beal, P. A.; Dervan, P. B. *Science* **1991**, *251*, 1360–1363.
(9) Stech, W. J.; Zon, G.; Egan, W.; Stec, B. *J. Am. Chem. Soc.* **1984**, *106*, 6077–6079.
(10) Connolly, B. A.; Potter, B. V. L.; Eckstein, F.; Pingoud, A.; Grothjahn, L. *Biochemistry* **1984**, *23*, 3443–3453.
(11) Nielsen, J.; Brill, W. K.; Caruthers, M. H. *Tetrahedron Lett.* **1988**, *29*, 2911.
(12) Löschner, T.; Engels, J. W. *Nucleosides Nucleotides* **1988**, *7*, 729–732.
(13) Sood, A.; Shaw, B. R.; Spielvogel, B. F. *J. Am. Chem. Soc.* **1990**, *112*, 9000–9001.
(14) Matteucci, M. *Tetrahedron Lett.* **1990**, *31*, 2385–2388.
(15) Coull, J. M.; Carlson, D. V.; Weith, H. L. *Tetrahedron Lett.* **1987**, *28*, 745–748.
(16) Stirchak, E. P.; Summerton, J. E.; Weller, D. D. *J. Org. Chem.* **1987**, *52*, 4202–4206.
(17) Cormier, J. F.; Ogilvie, K. K. *Nucleic Acids Res.* **1988**, *16*, 4583–4594.
(18) Huang, Z.; Schneider, K. C.; Benner, S. A. *J. Org. Chem.* **1991**, *56*, 3869–3882.
(19) Schneider, K. C.; Benner, S. A. *Tetrahedron Lett.* **1990**, *31*, 335–338.

0002-7863/92/1514-1895$03.00/0

Scheme I. Schematic Comparison of DNA (**1**) and PNA (**2**)[a]

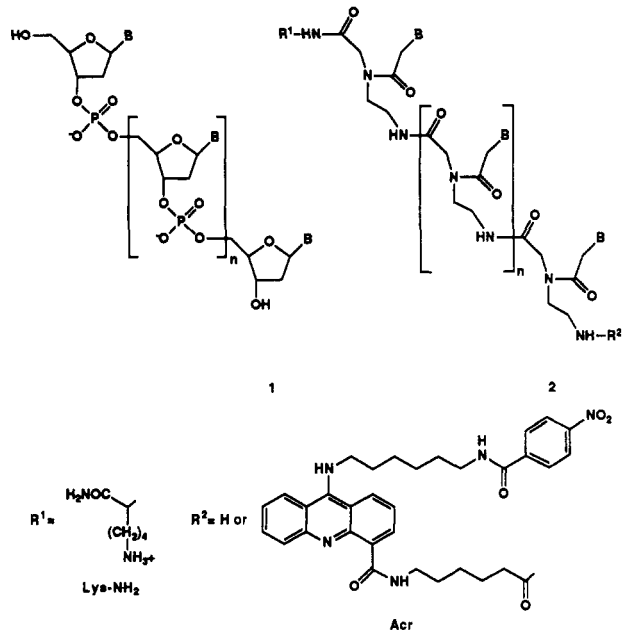

[a] **2a**, R^1 = Lys-NH_2, R^2 = H, n = 4; **2b**, R^1 = Lys-NH_2, R^2 = H, n = 6; **2c**, R^1 = Lys-NH_2, R^2 = H, n = 8; **2d**, R^1 = Lys-NH_2, R^2 = Acr, n = 8.

Scheme II[a]

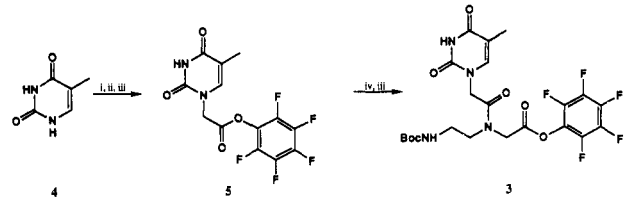

[a] (i) $BrCH_2CO_2CH_3$, K_2CO_3 in DMF, 24 h. (ii) Aqueous NaOH reflux 10 min. (iii) PfpOH, DCC in DMF, 3 h. (iv) BocNH-$(CH_2)_2NHCH_2CO_2H$,[29] Et_3N in DMF, 1 h.

consisting of (2-aminoethyl)glycine units and nucleobase attachments via methylenecarbonyl linkers could be used (**2**, Scheme I). Such a backbone would be homomorphous with the deoxyribose phosphate backbone of DNA with a high degree of constrained conformational flexibility due to the two amido groups per unit. Thymine was chosen as the nucleobase since it has no exocyclic amino group which might need protection. However, the design should allow relatively simple expansion into the other natural nucleobases as well as to other ligands of interest.

The preparation of the Boc-protected pentafluorophenyl ester of the thyminyl monomer (Boc-Taeg-OPfp, **3**) is outlined in Scheme II, and the PNAs are synthesized by Merrifield's solid-phase approach[20,21] employing a single-coupling protocol with 0.1 M Boc-Taeg-OPfp in 30% (v/v) DMF in CH_2Cl_2. To obtain C-terminal amides, the protected PNAs were assembled on a (4-methylbenzhydryl)amine resin (initially loaded with 0.28 mmol of Boc-L-Lys(ClZ) per gram resin).[22] The progress of the PNA synthesis was monitored throughout by quantitative ninhydrin analysis,[23] which showed that all couplings proceeded with an efficiency of ≥99%, except for coupling number 9 which gave 94%. The free PNAs were released from the resin with anhydrous HF under standard conditions.

The lysine included at the C-terminal diminished PNA self-aggregation and allowed the determination of overall efficiency by amino acid analysis. The H-T_{10}-Lys-NH_2 (**2c**) is readily soluble in water: more than 5 mg/mL.

Table I

PNA	DNA	T_m[a]
H-T_6-Lys-NH_2 (**2a**)	$(dA)_6$	31
H-T_8-Lys-NH_2 (**2b**)	$(dA)_8$	52
H-T_{10}-Lys-NH_2 (**2c**)	$(dA)_{10}$	72[d] (a)
H-T_{10}-Lys-NH_2 (**2c**)	$(dA)_{10}$	72[b]
H-T_{10}-Lys-NH_2 (**2c**)	$(dA)_{10}$	73[c]
H-T_{10}-Lys-NH_2 (**2c**)	$(dA)_5(dG)(dA)_4$	59[d] (b)
H-T_{10}-Lys-NH_2 (**2c**)	$(dA)_2(dG)(dA)_2(dG)(dA)_4$	46[d] (c)
Acr-T_{10}-Lys-NH_2	$(dA)_{10}$	86

[a] The melting temperatures of the hybrids were determined on a Gilford Response apparatus. The following extinction coefficients were used: A, 15.4, T, 8.8, and G, 11.7 mL/μmol·cm for both normal deoxyoligonucleotides and PNA. The solutions were 10 mM in phosphate, 10 mM in $MgCl_2$, 140 mM in NaCl, and pH 7.4, unless otherwise stated. 0.3 OD_{260}/mL of **2c** (for **2b** 0.24 OD_{260}/mL and for **2a** 0.18 OD_{260}/mL) was hybridized with 1 equiv of the other strand (using the extinction coefficients above for both PNA and DNA) by heating to 90 °C for 5 min, cooling to room temperature, and storing for 30 min followed by storage at 5 °C for at least 30 min. The melting curves were recorded in steps of 0.5 °C/min. The T_m values were determined from the maximum of the first derivative of the plot of A_{260} versus temperature. [b] 0 mM $MgCl_2$, 0 mM NaCl. [c] 0 mM $MgCl_2$, 500 mM NaCl. [d] The melting curves for a, b, and c are shown in Figure 1.

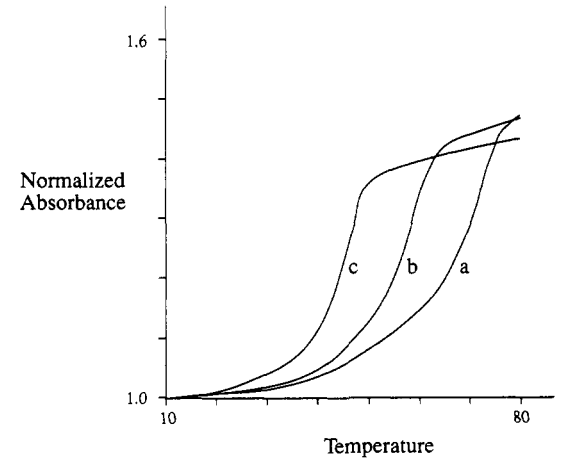

Figure 1. Melting curves of the H-T_{10}-Lys-NH_2 (**2c**)/$(dA)_{10}$ (a), H-T_{10}-Lys-NH_2 (**2c**)/$(dA)_5(dG)(dA)_4$ (b), and H-T_{10}-Lys-NH_2 (**2c**)/$(dA)_2(dG)(dA)_2(dG)(dA)_4$ (c) hybrids.

Other ligands are easily attached to the N-terminal. Thus, the photonuclease/intercalator ligand 6-[[[9-[[6-(4-nitrobenzamido)hexyl]amino]acridin-4-yl]carbonyl]amino]hexanoyl[24] was inserted at the N-terminal via its Pfp ester in >95% yield to give **2d**. The oligomers were all purified by HPLC and shown to have the expected molecular mass by plasma desorption mass spectrometry.

The PNA–DNA binding was examined by T_m measurements (Table I), giving well-defined melting curves (Figure 1) with T_m values much higher than those of the corresponding DNA/DNA duplexes and a relationship between T_m and length showing a ΔT_m of ~10 °C per molecular unit.

These results show that base stacking takes place and strongly indicate that PNA forms hybrids with complementary DNA. This should result in lower T_m values for DNA containing mismatches, which also turned out to be the case (Table I). The observation that the Acr-T_{10}-Lys-NH_2 (**2d**)/$(dA)_{10}$ melts even higher than the corresponding H-T_{10}-Lys-NH_2 (**2c**)/$(dA)_{10}$ indicates that the acridine intercalates between base pairs or is stacked at the end. The linear increase of T_m with length indicates that the electrostatic contribution from the positive charges to the binding is of minor importance (note that H-T_n-Lys-NH_2 is positively charged

(20) Merrifield, R. B. *J. Am. Chem. Soc.* **1963**, *85*, 2149–2154.
(21) Merrifield, B. *Science* **1986**, *232*, 341–347.
(22) Pietta, P. G.; Marshall, G. R. *J. Chem. Soc. D* **1970**, 650–651.
(23) Sarin, V. K.; Kent, S. B. H.; Tam, J. P.; Merrifield, R. B. *Anal. Biochem.* **1981**, *117*, 147.
(24) Egholm, M.; Christensen, L.; Nielsen, P. E.; Buchardt, O. Manuscript in preparation.

at both terminals at neutral pH; cf. Scheme I). As expected, the T_m values for PNA/DNA hybrids were little affected by changes in ionic strength (Table I).

The stoichiometry was determined by UV–titration curves to be 2:1 (2 PNA:1 DNA), as expected for a nonionic oligothymine derivative.[25-27]

By extending our findings to other nucleobases, a study that is currently under way, it may be possible to design reagents which recognize any sequence in single- or double-stranded DNA.[28]

Acknowledgment. This work was supported by the Danish Natural Science Research Council and The Benzon Foundation. Ms. Vivi Hedeboe and Ms. Annette W. Jørgensen are thanked for skilled technical assistance.

Supplementary Material Available: Experimental procedures for compounds **4–6** (3 pages). Ordering information is given on any current masthead page.

(25) Miller, P. S.; Fang, K. N.; Kondo, N. S.; Ts'o, P. O. P. *J. Am. Chem. Soc.* **1971**, *93*, 6657–6665.
(26) Miller, P. S.; Yano, J.; Yano, E.; Carroll, C.; Jayaraman, K.; Ts'o, P. O. P. *Biochemistry* **1979**, *18*, 5134–5143.
(27) Letsinger, R. L.; Bach, S. A.; Eadie, J. S. *Nucleic Acids Res.* **1986**, *14*, 3487–3499.
(28) The affinity for $(dA)_{10}$ of H-PNA-T_{10}-LysNH$_2$ is so high that it displaces the $(dT)_{10}$ part of the opposite strand in a 248 base pair double-stranded DNA fragment with an inserted $d(A)_{10}/d(T)_{10}$. Nielsen, P. E.; Egholm, M.; Berg, R. H.; Buchardt, O. *Science* **1991**, *254*, 1497–1500.
(29) Heimer, E. P.; Gallo-Torres, H. E.; Felix, A. M.; Ahmad, M.; Lambros, T. J.; Scheidl, F.; Meienhofer, J. *Int. J. Pept. Res.* **1984**, *23*, 203–211.

Intramolecular Energy Transfer in the Inverted Region

D. Brent MacQueen, John R. Eyler, and Kirk S. Schanze*

Department of Chemistry
University of Florida
Gainesville, Florida 32611-2046

Received October 28, 1991

Quantum mechanical theories of nonradiative transitions such as electron transfer (ET), nonradiative excited-state decay, and triplet–triplet (exchange) electronic energy transfer (E_nT) predict that when the process is strongly exothermic, the rate will increase as the driving force decreases.[1-4] This "inverted" rate–driving force dependence has been well-established for nonradiative excited-state decay and for both inter- and intramolecular ET.[5-14] By contrast, relatively few examples exist which provide clear evidence for the inverted effect for E_nT.[15,16]

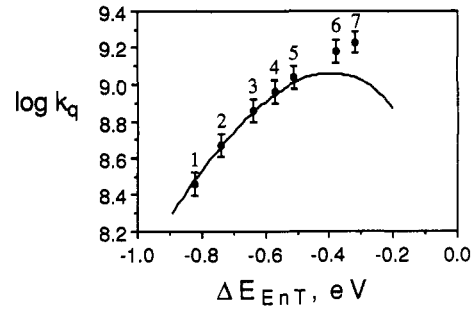

Figure 1. Plot of k_q vs ΔE_{EnT} for the series of (b)ReAn complexes in 2-methyltetrahydrofuran solution at 298 K (1 = tmb, 2 = dmb, 3 = bpy, 4 = 4-dab, 5 = 5-dab, 6 = deb, 7 = bpz). ΔE_{EnT} values were determined using the expression given in footnote 21. Error bars on k_q are estimated as ±15%. The solid line was calculated using eq 2 with the parameters listed in the text.

Series of d^6 transition-metal complexes with metal-to-ligand charge transfer (MLCT) excited states afford unique opportunities to study thermodynamic–kinetic relationships for ET and nonradiative excited-state decay.[5,6,9,11,17] This is because the energy of the MLCT state (E_{MLCT}) can be readily tuned by varying ligands; and by using a series of structurally related ligands, electronic coupling terms are not strongly perturbed.[5,6] We have recently applied this technique to study E_nT from the $d\pi$ (Re) $\rightarrow \pi^*$ (diimine) MLCT chromophore to the anthracene (An) chromophore in the series of complexes (b)ReAn.[18] In these "bichromophores", the MLCT excited state of the (b)Re^I(CO)$_3$ donor undergoes strongly exothermic E_nT to the lowest triplet state of the An acceptor via the Dexter exchange mechanism.[19] The results of this study provide clear evidence for an inverted dependence of the rate of E_nT (k_{EnT}) on ΔE_{EnT}.

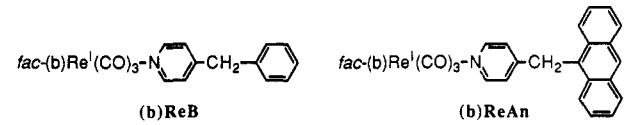

Photoexcitation of the (b)Re(CO)$_3$ chromophore in the near-UV region populates diimine-based $^1(\pi,\pi^*)$ and ^{1}MLCT excited states which relax rapidly ($k > 10^{11}$ s^{-1}) with unit quantum efficiency to the luminescent ^{3}MLCT state.[20] Strong, relatively long-lived MLCT luminescence is observed from each of the (b)ReB model complexes which do not contain the An chromophore. By contrast, only very weak, short-lived MLCT emission is observed from the (b)ReAn complexes. The dominant mode for MLCT quenching is E_nT:

$$*[(b^{\bullet-})Re^{II}(CO)_3Py]CH_2An \xrightarrow[\Delta E_{EnT}]{k_{EnT}} (b)Re^{I}(CO)_3PyCH_2[^3(An)]^* \quad (1)$$

That MLCT quenching is due principally to intramolecular E_nT is supported by several lines of evidence. First, E_nT is strongly to moderately exothermic for each complex.[21] Second, competitive

(1) Robinson, G. W.; Frosch, R. P. *J. Chem. Phys.* **1963**, *38*, 1187.
(2) Ulstrup, J.; Jortner, J. *J. Chem. Phys.* **1975**, *63*, 4358.
(3) Henry, B. R.; Siebrand, W. In *Organic Molecular Photophysics*; Birks, J. B., Ed.; Wiley: New York, 1973; Vol. 1, p 153.
(4) Orlandi, G.; Monte, S.; Barigelletti, F.; Balzani, V. *Chem. Phys.* **1980**, *52*, 313.
(5) (a) Caspar, J. V.; Kober, E. M.; Sullivan, B. P.; Meyer, T. J. *J. Am. Chem. Soc.* **1982**, *104*, 630. (b) Meyer, T. J. *Prog. Inorg. Chem.* **1983**, *30*, 389. (c) Worl, L. A.; Duesing, R.; Chen, P. Y.; Della Ciana, L.; Meyer, T. J. *J. Chem. Soc., Dalton Trans.* **1991**, 849.
(6) Caspar, J. V. Ph.D. Dissertation, University of North Carolina, Chapel Hill, 1983.
(7) Miller, J. R.; Calcaterra, L. T.; Closs, G. L. *J. Am. Chem. Soc.* **1984**, *106*, 3947.
(8) Wasielewski, M. R.; Niemczyk, M. P.; Svec, W. A.; Pewitt, E. B. *J. Am. Chem. Soc.* **1985**, *107*, 1080.
(9) Chen, P.; Duesing, R.; Tapolsky, G.; Meyer, T. J. *J. Am. Chem. Soc.* **1989**, *111*, 8305.
(10) Fox, L. S.; Kozik, M.; Winkler, J. R.; Gray, H. B. *Science* **1990**, *247*, 1069.
(11) MacQueen, D. B.; Schanze, K. S. *J. Am. Chem. Soc.* **1991**, *113*, 7470.
(12) Miller, J. R.; Beitz, J. V.; Huddleston, R. K. *J. Am. Chem. Soc.* **1984**, *106*, 5057.
(13) Gould, I. R.; Ege, D.; Moser, J. E.; Farid, S. *J. Am. Chem. Soc.* **1990**, *112*, 4290.
(14) Ohno, T.; Yoshimura, A.; Mataga, N. *J. Phys. Chem.* **1990**, *94*, 4871.
(15) Murtaza, Z.; Zipp, A. P.; Worl, L. A.; Graff, D.; Jones, W. E., Jr.; Bates, W. D.; Meyer, T. J. *J. Am. Chem. Soc.* **1991**, *113*, 5113.
(16) Sigman, M. E.; Closs, G. L. *J. Phys. Chem.* **1991**, *95*, 5012.
(17) Juris, A.; Balzani, V.; Barigelletti, F.; Campagna, S.; Belser, P.; Von Zelewski, A. *Coord. Chem. Rev.* **1988**, *84*, 85.
(18) Diimine ligand (b) abbreviations: tmb = 4,4',5,5'-tetramethyl-2,2'-bipyridine; dmb = 4,4'-dimethyl-2,2'-bipyridine; bpy = 2,2'-bipyridine; 5-dab = 5,5'-bis(*N*,*N*-diethylcarbamido)-2,2'-bipyridine; 4-dab = 4,4'-bis(*N*,*N*-diethylcarbamido)-2,2'-bipyridine; deb = 4,4'-bis(carbethoxy)-2,2'-bipyridine; bpz = 2,2'-bipyrazine.
(19) Dexter, D. L. *J. Chem. Phys.* **1953**, *21*, 866.
(20) Schanze, K. S.; Pourreau, D. B.; Netzel, T. L. Unpublished results.
(21) The ΔE_{EnT} values were determined by $\Delta E_{EnT} = E_T(An) - E_{MLCT}$, where $E_T(An)$ is the energy of ^{3}An* and E_{MLCT} is defined in the text. $E_T(An)$ = 1.79 eV (ref 26), and the E_{MLCT} values were determined from emission spectra of the (b)ReB complexes as described in ref 6.

0002-7863/92/1514-1897$03.00/0